Analysis of Photovoltaic Performance Loss Rates of Six Module Types in Five Geographical Locations

Philip Ingenhoven, Giorgio Belluardo, George Makrides, George E. Georghiou, Paul Rodden, Lyndon Frearson, Bert Herteleer, Dario Bertani, and David Moser

***Abstract*—In this paper, the annual performance loss rates (PLRs) of five different grid-connected photovoltaic (PV) technologies based on outdoor field measurements were computed. The data used were collected in five different geographical locations covering five climatic zones. The PLR values were determined as absolute and relative measures for all sites and module types using seasonal time series decomposition using local regression. The results are very consistent and show a clustering of the PLR for each technology, provided some explainable outliers are removed. This allows the conclusion that in presence of properly sized and quality-driven systems, the influence of different climates on the degradation of PV modules is not very strong. In the first approximation, individual degradations rate values computed in a single climatic zone can be seen as representative for the technology in general. The reason for this is that for defects there is an associated activation energy, which has not been reached yet in the systems analyzed in this study.**

***Index Terms*—Climate dependence, performance loss rate (PLR), performance ratio (PR), photovoltaic (PV) degradation.**

I. Introduction

HISTORICAL performance data for photovoltaic (PV) systems on which to base technical risks yield assessments, and investment decisions are difficult to be accessed by all market players. Reasons for this difficulty are to be found in the tendency among systems operators, asset managers, PV plant owners, and component manufacturers to keep available performance data as confidential. Degradation trends can vary between PV plants depending on 1) the role quality plays during the design, engineering, procurement, and construction phase, 2) the quality of the monitoring system and logged data, and 3) the climate of the selected site. Jordan *et al.* [1] discussed the impact of climate on degradation rates, but their analysis failed in finding a significant climatic difference, which instead is shown in [2]. In all these analyses, the module manufacturer may vary, and in the calculated degradation rates, the inclusion of a few underperforming modules may significantly increase the probability of a lower system performance. In summary, from 1751 published studies for monocrystalline silicon (c-Si), the average degradation rate was calculated at 0.7%/year and the median at 0.5%/year, with the majority of studies published before 2000, whereas for 169 published studies for thin-film technologies the average and median were higher, at 1.5%/year and 1%/year, respectively, with the majority of studies published after 2000. These results did not include initial degradation (minimum three years of measurement data). Although the average for thin-films was 1.5%/year, the rates were spread from 0.2 to 4.2%/year, whereas for c-Si the rates were mainly concentrated around the median. With respect to climatic effects on degradation rate, it cannot be generalized that hotter climates necessarily lead to higher degradation for all products. However, from this study, it was obvious that climate and mounting configuration may lead to higher degradation in some PV products compared with others. In this paper, the analysis of the performance loss rate (PLR) is reported for five geographical locations using only data coming from PV plants with high-quality monitoring data available and a well-defined track record of failures and issues found in the field. At all sites, a database was kept to document the occurrence and duration of energy loss conditions for each monitored PV system. The main PV system outage conditions throughout the evaluation period included module, inverter, and balance of equipment breakdown, Operation&Maintenance (O&M) scheduled outages, and utility loss. Immediate actions were taken to mitigate all energy loss issues (replacement of modules, inverters, and balance of system (BOS) equipment), whereas the data acquired during the fault/outage period were filtered out from the performance loss estimation. The availability of field information allows for the exclusion of trends due to sudden component failures or other issues not related with long-term material degradation and hence to focus on the impact of climate on the PLR.

Manuscript received December 17, 2018; revised March 1, 2019 and April 6, 2019; accepted April 20, 2019. Date of publication May 22, 2019; date of current version June 19, 2019. The work of P. Ingenhoven, G. Belluardo, and D. Moser was supported by EURAC, which was cofunded by the Stiftung Südtiroler Sparkasse within the IEA-PVPS Task 13 network. The work of D. Bertani was supported by the RSE, which was funded by the Research Fund for the Italian Electrical System under the Contract Agreement between RSE S.p.A. and the Ministry of Economic Development stipulated on July 29, 2009 in compliance with the Decree of March 19, 2009. The work of P. Rodden, L. Frearson, and B. Herteleer was supported by Ekistica, which was funded by ARENA under IEA PVPS Task 13. *(Corresponding author: Philip Ingenhoven.)*

P. Ingenhoven, G. Belluardo, and D. Moser are with the Institute for Renewable Energy, EURAC Research, 39100, Bolzano, Italy (e-mail: philip.ingenhoven@eurac.edu; giorgio.belluardo@eurac.edu; david.moser@eurac.edu).

G. Makrides and G. E. Georghiou are with the University of Cyprus, Nicosia 1678, Cyprus (e-mail: makrides.georgios@ucy.ac.cy; geg@ucy.ac.cy).

P. Rodden, L. Frearson, and B. Herteleer are with the Ekistica, Connellan, NT 0870, Australia (e-mail: Paul.Rodden@ekistica.com.au; lyndon.frearson@ekistica.com.au; bert.herteleer@ekistica.com.au).

D. Bertani is with the RSE SpA, 20134 Milano, Italy (e-mail: dario.bertani@rse-web.it).

Color versions of one or more of the figures in this paper are available online at http://ieeexplore.ieee.org.

Digital Object Identifier 10.1109/JPHOTOV.2019.2913342

TABLE I
MONITORING PERIODS AT THE DIFFERENT SITES (YEARS)

	EURAC	UCY	DKASC	RSE Mil.	RSE Cat.
CdTe	6	8	4	6	-
c-Si	6	-	8 & 6	6	6
CIS	6	8	-	6	6
HIT	6	8	7	6	6
m-Si1	6	8	-	-	-
m-Si2	6	-	8	-	-

II. EXPERIMENTAL SET-UP

Monitoring data were collected at five different geographical locations managed by four different research institutions. Periodic calibrations and inspections of the sensors installed were performed to ensure good-quality measurements and reveal any departures from the real measurements. In total, six PV module types (same manufacturer/model) from five technologies were chosen to be compared among the sites. The technologies analyzed are c-Si and multicrystalline silicon, heterojunction silicon (HIT), cadmium telluride (CdTe), and copper indium selenide (CIS). Each of these are present in at least two different sites. In Table I, the technologies and their availability are summarized. The numbers in the table indicate the number of years the plants were monitored, which is equal to the number of years of operation of these modules at the time of submission. The systems were all grid connected using identical inverter types at each site in order to exclude the influence of different maximum power point tracking methods to the dc yield. The nominal power ratio (inverter PV array) of the inverter was slightly oversized (110%) in order to avoid clipping.

The PV test sites are located in Italy: Bolzano (EURAC), Milano (RSE), Catania (RSE); Cyprus: Nicosia at the University of Cyprus (UCY); and Australia: Alice Springs (Desert Knowledge Australia Solar Center (DKASC), maintained by Ekistica). In the following paragraphs, the different monitoring sites are briefly described and summarized in Table II.

A. EURAC—Bolzano

The data analyzed in this paper were collected from the PV outdoor test facility of Airport Bolzano Dolomiti (position ca. 46.46N, 11.33E, elevation: 262 m) located in South Tyrol, Italy [3]. The facility is located at the junction of the three valleys: Val d'Isarco, Val Sarentino, and Val d'Adige. In total, 26 PV arrays from 1 to 7 kWp of different module types (technology, manufacturer, and design) are installed at a fixed tilt of 30° and an orientation of 8.5° west of south. All arrays are installed within 100 m of the weather station and are exposed to similar horizon shading, however due to self-shading of the rows, some modules experience local shading in December. Dc-side electrical parameters of each array are measured every 15 min by commercial inverters assuring a good level of accuracy in dc current (I_{dc}) and dc voltage (V_{dc}), with an average difference from a dedicated system of less than 5% and less than 2%, respectively, decreasing at higher irradiance [4], [5]. The inverters are all from the same manufacturer (SMA) and errors due to different maximum power point tracking are assumed to be comparable between the different systems. Thus, the PLRs are deducible from the data collected this way. A dedicated meteo station collects data of global horizontal (G_{hor}), direct normal (G_{dir}), and diffuse (G_{dir}) irradiance as well as global plane-of-the-array irradiance (G_{POA}). Further wind speed (v_{wind}) and direction (α_{wind}) as well as ambient (T_{amb}) and module (T_{mod}) temperatures are measured. The acquisition frequency is 1 min, which is then averaged on a 15-min time interval, to match the electrical data. The sensors are systematically cleaned and periodically calibrated in order to comply with the standard IEC61724:1998 [6]. During the investigated time, the pyranometers were calibrated three times (every two years). The average sensitivity was 8.62 microV/W/m^2 and st.dev 0.07 microV/W/m^2 (0.81% relative). No clear deviation/trend was observed in the sensitivity value (clear increase/decrease). Electrical data have been recorded since August 2010, whereas weather data are available from February 2011.

B. UCY Nicosia

The PV systems have been monitored since June 2006. Both meteorological and PV system measurements are acquired and stored using an advanced measurement platform. The platform comprises of irradiance, weather, and electrical sensors, connected to a central data-logging system that stores data at a resolution of 1-s and accumulation steps of 15-min averages. The meteorological measurements include G_{POA}, T_{amb}, v_{wind}, and α_{wind} [7]. The PV operational data include the array I_{dc}, V_{dc}, P_{dc}, P_{ac}, and T_{mod}. The secondary standard pyranometer installed in the POA and used in this investigation for the irradiance measurements had an initial calibration value that was 11.84 V/Wm^2 and after four years the new calibration sensitivity value was 11.86 V/Wm^2, which effectively results in an absolute percentage error of -0.17%. Periodic cleaning of the dome of the pyranometer was further performed when the PV arrays were cleaned too. The main sources of uncertainty in the outdoor PV performance evaluations, due to the instrumentation were also investigated. The global irradiance was measured using a thermopile pyranometer in the spectral range of 310–2800 nm with a 2% expected daily uncertainty. In practice, since the expected daily uncertainty of the pyranometer is based on a particular daily profile of irradiance, solar path, and ambient temperature variations of a particular location, the application of the sensor in other climatic conditions renders the uncertainty of the pyranometer, a function of many variables such as directional errors in zenith and azimuth directions, cosine response, temperature sensitivity, and level of irradiance. For a secondary standard instrument, the expected maximum errors are $\pm 2\%$ for the daily total error, described by the World Meteorological Organization, because some response variations cancel out each other if the integration period is long. To further reduce the remaining errors, the conversion of voltage to irradiance, obtained from the calibration sheet of the instrument, is specified and can be important as a bias. In addition, the response time of this pyranometer is 5 s (for 95% response), which is longer than the PV module response time and the 1-s data-logging interval. This introduces an additional uncertainty contribution in the measurements that has not been considered in this investigation. Furthermore, the pyranometer was also ventilated and heated, to avoid incorrect measurements caused by dew and snow.

C. DKASC—Alice Springs Australia

The DKASC is a demonstration facility for commercialized solar technologies operating in the arid solar conditions of Alice Springs, Central Australia (23.7618° S, 133.8749° E).

TABLE II
MONITORING DEVICES

Parameter	EURAC Manufacturer / Model	UCY Manufacturer / Model	DKASC Manufacturer / Model	RSE Manufacturer / Model
Data acquisition	SMA NI / Sunny Webbox Crio	Delphin / TopMessage	dataTaker / DT80	Teamware / E2M-PV
Ambient temperature (T_{amb})	Thies Clima / Thermo-Sensor-compact	Theodor Friedrich / 2030	Vaisala / MPT45A	Teamware / NTC Thermistor
Module temperature (T_{mod})	Heraeus / PT100	Heraeus / PT100	N/A / N/A	Teamware / NTC Thermistor
Global horizontal irradiance (G_{hor})	Kipp Zonen / CMP11	N/A N/A	Delta-T / SPN 1	Kipp Zonen / CMP 11
Direct normal irradiance (G_{dir})	Kipp Zonen / CHP1	Kipp Zonen / CH 1	Delta-T / SPN 1	N/A / N/A
Diffuse irradiance (G_{dif})	Kipp Zonen / CHP1	Kipp Zonen / CH 1	Delta-T / SPN 1	N/A / N/A
Global Tilted Irradiance (G_{POA})	Kipp Zonen / CMP11	Kipp Zonen / CM 21-CV 2	From 2015 Delta-T / SPN 1	IKS Photovoltaic / ISET sensor
DC voltage (V_{dc})	SMA / SunnyBoy	Custom made / Potential divider	SMA / Sunny Mini Central (not stored)	Custom made / Potential divider
DC current (I_{dc})	SMA / SunnyBoy	Custom made / Shunt resistor	SMA / Sunny Mini Central (not stored)	Custom made / Shunt resistor
DC power (P_{dc})	SMA / SunnyBoy	Delphin / TopMessage	SMA / Sunny Mini Central	Teamware / DCM-PV
AC power (P_{ac})	SMA / SunnyBoy	NZR / AAD1D5F	Ion / 7550, CT 5/100	Teamware / E2M-PV
Wind speed (v_{wind})	Gill Instruments / WindSonic	Theodor Friedrich / 4034	Vaisala / WS425	LSI / DNA727
Wind direction (α_{wind})	Gill Instruments / WindSonic	Theodor Friedrich / 4122	Vaisala / WS425	LSI / DNA727
	N/A / N/A	N/A / N/A	Vaisala / HMP45A	N/A / N/A
	N/A / N/A	N/A / N/A	Vaisala / TB3A	N/A / N/A

More than 30 arrays and multiple module technologies are monitored. Monitoring started in 2008, with technologies continuing to be added. All systems discussed in this paper are connected to identical SMA Sunny Mini Central 5-kW inverters, and the PLRs are therefore comparable between the different systems. Temperature and irradiance data are measured with a dedicated weather station. Pyranometers are cleaned on a weekly basis per manufacturer and industry best practices and regularly calibrated. Data are measured at 10-s intervals, with the averaged 5-min data stored on DKASC's public-facing repository, and the 5-min averaged data is used in this paper. The modules discussed in this paper are at a 20° tilt angle, due north. The arrays are subject to morning and/or evening shading from surrounding trees.

The plane of array irradiance G_{POA} was computed using geometrical reconstruction

$$G_{\mathrm{dir}} = \frac{G_{\mathrm{hor}} - G_{\mathrm{dif}}}{\sin(\alpha)} \tag{1}$$

$$G_{\mathrm{POA}} = G_{\mathrm{dir}} \cdot \cos(\theta) + G_{\mathrm{dif}} \cdot \frac{1}{2} \cdot (1 + \cos(20^\circ)) \tag{2}$$

$$+ \ \rho \cdot G_{\mathrm{hor}} \cdot \frac{1}{2} \cdot (1 - \cos(20^\circ)) \tag{3}$$

where G_{dir}, G_{dif}, and G_{hor} are the direct, diffuse, and global horizontal irradiance, respectively, and where α is the sun elevation and θ the incidence angle of the irradiance on the POA. With the introduction of a new POA pyranometer in 2015, it was possible to find a more accurate value for the ground albedo ρ and the computed values for G_{POA} were calibrated with the measured data.

For the P_{ac}, 5-min average values are used. Over a 5-min period, 1 s readings are averaged . This is measured with a Class 0.2 m with $\pm 0.2\%$ accuracy (Ion 7550, CT: 5/100). To be able to compare these values, several months of P_{dc} data were monitored and compared with the P_{ac} data. From this, it was possible to recover the P_{dc} for the complete time series.

D. RSE—Milano and Catania

RSE operational data analyzed in this paper have been acquired in two different test facilities, located in northern and southern Italy, respectively. The first one is located in RSE main headquarters in Milan (Italy; 45° 27'N - 9° 11'E; 127 m a.s.l.) and its climate is classified as Cfa (Humid subtropical climate) according to Koppen classification. The southern facility is located in Catania (37° 30'N - 15° 05'E; 7 m a.s.l.), hosted by Enel Green Power's Innovation Hub, and its climate is classified as Csa (Hot-summer Mediterranean climate). Each facility is composed of eight experimental PV plants, with an average nominal power of 1.5 kWp, with different PV technologies (Si-poly, Si-mono, CdTe, CIS, amorphous silicon, etc.) and with inverters of the same manufacturer (SMA). For each PV technology, modules of both plants have the same manufacturer, model, and production batch. They have been operational since 2009 and are installed with fixed inclination/orientation (30°, south) on ground-mounted structures. Operational monitoring is carried out through a dedicated monitoring system, which consists of a network of remote measurement units installed at PV systems, with independent units for meteorological measurements (horizontal and plane-of-array solar radiation and ambient and back-of-the-module temperatures) and electrical measurements. The latter are performed with accuracy below 1% (I_{dc}, P_{dc}, and P_{ac}). Solar radiation measurements are acquired through periodically calibrated Silicon reference cells (2% measurement uncertainty $+1\%$ on the reading), while temperatures are measured by a negative temperature coefficient (NTC) thermistor (accuracy ± 1 °C). Each measurement is acquired every 10-s and then resampled as 15-min averages, data are then sent through a wireless connection to a central database where they are stored.

E. Climatic Condition at the Different Sites

The monitored PV arrays are degrading under different climatic conditions. The climatic conditions are classified according to the updated Köppen–Geiger classification [8]. The climatic conditions at the five different sites belong to arid and temperate zones. Including subclassifications, such as steppe and desert in arid zones in Cyprus and Alice Springs, and warm, hot, and dry summers in the temperate zones for the Italian sites, the five sites are located in five different climatic conditions. More detailed climatic information can be found in Table III.

III. COMPUTATION OF THE PLR

Before commencing to the PLR analysis, data quality routines (DQRs) were applied to the acquired data to ensure data validity for the subsequent PLR evaluation. Thus, the recorded data were thoroughly checked for consistency and gaps before any additional analysis was conducted. In particular, the developed DQRs run algorithms for detecting missing and erroneous data and operate filters to identify outliers and outages and remove

TABLE III
CLIMATIC INFORMATION ABOUT THE DIFFERENT TEST SITES

			Mean Temp. [°C] Winter		Spring		Summer		Autumn		Mean Monthly Precipitation [mm] Winter	Spring	Summer	Autumn
	Climate Zone	Short Description	Min	Max	Min	Max	Min	Max	Min	Max				
EURAC	Cfb	Temperate Warm Summer	-3.7	7.3	5.3	19.0	14.3	28.0	5.7	18.3	26.3	60.0	88.7	59.7
UCY	BSh	Arid Steppe hot	5.6	16.1	9.9	23.6	19.3	35.0	13.9	27.5	58.7	25.7	2.7	22.7
DKASC	BWh	Arid Desert hot	4.8	21.0	14.7	31.2	21.1	36.0	12.9	28.3	11.7	20.4	40.4	24.6
RSE MI	Cfa	Temperate Hot Summer	-0.3	7.0	7.7	17.7	17.0	28.0	9.0	17.7	56.5	78.7	74.1	97.4
RSE CA	Csa	Temperate Dry Summer	5.7	16.3	9.0	20.7	18.0	30.7	13.7	24.7	71.3	33.3	6.7	71.0

the identified out of range and erroneous values and reconstruct the data set.

The PLR is computed using the monthly performance ratio (PR). The PR $\mathrm{PR}_{\mathrm{month,AC}}$ over a specified period is defined in the IEC 61724:1 standard [6] as the ratio of the final yield Y_f (i.e., the generated ac-energy per kW of installed PV array) and the reference yield Y_r (i.e., the ratio of POA irradiance and irradiance at STC conditions) over that period. The different yields are defined as

$$Y_f = \sum_{\text{month}} \frac{P_{\mathrm{AC}}(t)}{P_n},\ Y_r = \sum_{\text{month}} \frac{G_{\mathrm{POA}}(t)}{G_{\mathrm{ref}}},\ Y_a = \sum_{\text{month}} \frac{P_{\mathrm{DC}}(t)}{P_n} \tag{4}$$

where Y_a is the array yield, i.e., the generated dc-energy per kW of installed PV array. For the purposes of this paper, only the dc-energy is used in place of ac-energy, thus leading to a slightly modified version of the PR

$$\mathrm{PR}_{\mathrm{month,DC}} = \frac{Y_a}{Y_r}. \tag{5}$$

This definition makes sure that only effects of the PV arrays are taken into account. In the above-mentioned definition of $\mathrm{PR}_{\mathrm{month,AC}}$, as defined in [6], effects due to possible inverter degradation influence the results, hence the usage of (5).

The PLR is computed using the time series decomposition method as described in [9]. The original $\mathrm{PR}_{\mathrm{monthly}}$ time series is split into three parts

$$\mathrm{PR}_{\mathrm{monthly}}(t) = T_t + S_t + R_t \tag{6}$$

where T describes the long-term trend of the time series, S the seasonality, and R the remainder. For the classical additive series decomposition, the trend T_t is found using a symmetrical 12-month moving average. The seasonality and the remainder are found following [10]. Because of the usage of the moving average to find the trend, the time series misses 6 months in the beginning and the end of the time series, leaving the trend series 12 months shorter than the original series. There are methods to overcome this disadvantage [e.g., autoregressive integrated moving average (ARIMA) and the seasonal-trend decomposition using local regression (STL)]. Phinikarides *et al.* [11] used ARIMA and STL to find an estimation of the trend also for the first and last 6 months of the time series. In this paper, only the STL method [12] is considered. The STL method uses various loops of local regression using locally weighted scatter-plot smoothing, for details see [10] and [12].

A linear fit is used on the trend T_t to define the performance loss estimation for both time series decompositions

$$T_t = a \cdot t + b. \tag{7}$$

The relative PLR is estimated according to

$$\mathrm{PLR}_{\mathrm{rel}} = \frac{12a}{b} \tag{8}$$

from the fitting parameters, with the uncertainty of

$$u_{\mathrm{PLRrel}} = \sqrt{\left(\frac{12}{b}\right)^2 \cdot u_a^2 + \left(\frac{12a}{b^2}\right)^2 \cdot u_b^2} \tag{9}$$

where the uncertainties of the fitting constants ($u_{a/b}$) are taken from the curve fitting toolbox of MATLAB [13]. The STL decompositions were performed using the time series package [14] of the software R [15]. Note that the definition of the PLR in (8) is the relative PLR as it takes into account the starting value of the PR ($\mathrm{PR}_0 = b$). Alternatively, it is possible to define the PLR absolutely as

$$\mathrm{PLR}_{\mathrm{abs}} = 12a \tag{10}$$

with the same parameters as above. Here, the errors are simply computed via

$$u_{\mathrm{PLRabs}} = 12 \cdot u_a. \tag{11}$$

In the literature, examples for the usage of both definitions exist. Kyprianou *et al.* [16] derived the degradation only from the trend's slope, thus using the absolute definition of the performance loss. The relative definition is used by, e.g., Ingenhoven *et al.* [9] and Belluardo *et al.* [17]. Many publications such as [1] do not define how the degradation rates are computed and collect data from various sources without going into detail on this topic. Thus, the authors would like to stress the importance of a clear definition of the PLR and the need for its standardization, as the two quantities can vary substantially. Results for both options are reported in Table IV.

IV. RESULTS

In the following section, the PLR results of the different technologies are discussed. Fig. 1 shows an overview of the relative PLR values for all investigated technologies. The PLR values of all technologies for both absolute and relative PLRs are given in Table IV. In the detailed discussion of the results, only the relative PLR is used.

A. Cadmium Telluride

For CdTe, a high PLR was observed in all installations but one over the evaluation period. All but one installation show very large relative performance losses, on average -1.92% /year. The installation in Australia shows a much lower PLR of about -1%. Data were collected for only four years there. This extraordinary result might be explained as being due to the shorter monitoring time rendering the data as not fully comparable [18]. However,

TABLE IV
COMPARISON OF ABSOLUTE AND RELATIVE PLR VALUES

	EURAC		UCY		DKASC		RSE Mil.		RSE Cat.		Mean	
	PLR rel	PLR abs	PLR rel	PLR abs	PLR rel	PLR abs	PLR rel	PLR abs	PLR rel	PLR abs	PLR rel	PLR abs
CdTe	-1.87 ± 0.08	-1.70 ± 0.07	-2.30 ± 0.04	-2.04 ± 0.04	-1.09 ± 0.11	-1.02 ± 0.11	-2.43 ± 0.06	-2.21 ± 0.05	-	-	-1.92 ± 0.60	-1.74 ± 0.52
c-Si	-0.95 ± 0.12	-0.90 ± 0.11	-	-	-0.80 ± 0.04	-0.68 ± 0.04	-2.21 ± 0.06	-2.14 ± 0.06	-0.63 ± 0.04	-0.59 ± 0.04	-1.15 ± 0.63	-1.08 ± 0.62
	-	-	-	-	-1.17 ± 0.10	-1.11 ± 0.09	-	-	-	-	-	-
CIS	-4.73 ± 0.23	-3.10 ± 0.15	-2.57 ± 0.04	-2.43 ± 0.03	-	-	-2.14 ± 0.07	-1.59 ± 0.05	-1.37 ± 0.06	-1.00 ± 0.04	-2.91 ± 1.33	-2.17 ± 0.86
	-3.72 ± 0.21	-2.73 ± 0.15		-	-	-	-	-	-	-	-	-
HIT	-0.86 ± 0.09	-0.80 ± 0.08	-0.78 ± 0.04	-0.70 ± 0.04	-1.66 ± 0.08	-1.59 ± 0.08	-1.67 ± 0.04	-1.59 ± 0.04	-0.97 ± 0.07	-0.89 ± 0.07	-1.19 ± 0.44	-1.11 ± 0.44
m-Si1	-0.60 ± 0.10	-0.55 ± 0.09	-1.23 ± 0.02	-1.09 ± 0.02	-	-	-	-	-	-	-0.91 ± 0.45	-0.82 ± 0.38
m-Si2	-0.90 ± 0.09	-0.80 ± 0.08	-	-	-1.05 ± 0.04	-0.95 ± 0.04	-	-	-	-	-0.98 ± 0.11	-0.87 ± 0.11

Uncertainty are calculated from the fitting procedures [%/year].

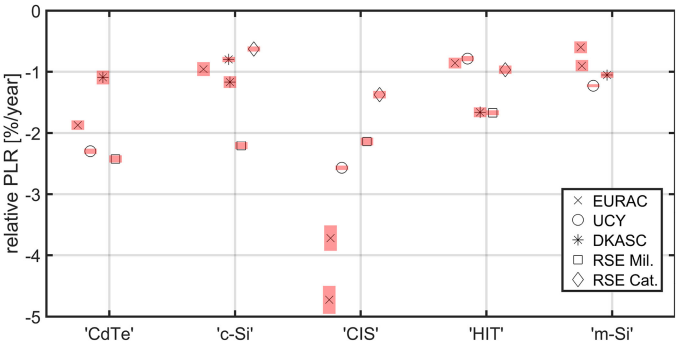

Fig. 1. Relative PLR values for all technologies and sites. For clarity only relative PLR values are shown in this figure. To find the absolute values see Table IV.

comparing this result with earlier results from the test site at EURAC [17] where the performance was analyzed over three years and showed −1.4% loss/year, this may indicate that there is a step wise degradation of CdTe modules. The analysis of changing PLR over time will be performed in a future study.

B. Monocrystalline Silicon

For c-Si, the average relative performance loss is −1.15%/year. For most installations, the loss rate is lower than that (from −0.63 to −0.95%/year). Only the installation from RSE in Milan shows—with a relative PLR of −2.21%/year—a unusually high PLR. To better understand this result, an *I–V* analysis (corrected to standard test conditions) of the string in question was performed that showed an average power decline of −2.3%/year (from 1200 to 1036 W in six years). The fill factor dropped from 79.9% to 73.8% in the same time. The current declined from 5.87 to 5.58 A, whereas the voltage stayed almost the same (256.0 to 251.6 V). The decline in power is mainly manifested in the decline in current and fill factor. However, thermo-graphic imaging of the string in questions did not reveal evident defect/degradation phenomena.

C. Copper Indium Selenide

The CIS technology of the manufacturer of these specific modules performs very badly with an average relative PLR of −2.91%/year. Loss rates as large as −4.73%/year were measured at EURAC, whereas the installation in Catania only loses a moderately large −1.37%/year. The CIS technology shows a large initial degradation and a large influence of metastable effects [19], which can explain the large performance loss to some extent. The very large performance loss at EURAC might be caused by partial shading present during the morning and evening hours in winter in the mountainous environment. Reverse stress caused by partial shading causes metastability in CIS modules [20]–[22], which might be the reason for the high degradation at EURAC. The manufacturer of these modules has since left the PV industry.

D. Heterojunction

The relative performance loss of the HIT technology is −1.19%/year, however two distinct groups can be identified. EURAC, UCY, and RSE Catania perform well with a PLR around −1%/year whereas DKASC and RSE Milan show considerably larger losses at about −1.67%/year. At these installation, the HIT modules show significant encapsulant browning, which is not present in the other installations.

E. Multicrystalline Silicon

The m-Si technologies show a low PLR however with a wide range. The average relative PLR is −0.91 and −0.98%/year for the two different module types monitored. For m-Si1, the difference between the values varies from −0.6 to −1.23%/year, which is a very large relative difference. However, as there were data from only two sites for the respective technologies, it is difficult to compare these. The picture in the second technology is much more uniform.

As mentioned in Section III, there are two ways of defining the performance loss as shown in Table IV. The difference in the definition is weighting with the initial PR value. It can be seen that for technologies with a high initial PR values, the difference between the two values is small. This is the case for all silicon-based technologies and CdTe. The factor between absolute and relative PLR is from 0.9 to 0.93 on average. This factor depends on the y-intercept of the regression of the PR. For the CIS technology, the difference is higher and the factor is 0.75 on average. As long as the exact definition is given, both definitions are valid indicators for the performance loss. However, the relative PLR enables the estimation of other performance parameters such as the yield as only the initial yield needs to be known for an approximate estimation of future yields.

F. Results in Literature

In the literature, there are few publications related with the direct comparison of the effect of different climates. A study of performance degradation in India [23] shows that a slight difference exists in the degradation rates for different climates. According to the study, the degradation rates are higher in hot climates than

in cooler climates. However, the difference is small and the error bars are overlapping. Further investigation is needed.

Two studies analyzed the climatic effect on the degradation rates with similar findings. A study [24] in which three example climates (Mediterranean, hot and humid, and hot and dry) were modeled found that after 30 years in all investigated zones, the overall degradation did not differ in values. Differences showed up after a longer period. This could be explained with the activation energy that is necessary for a degradation mode to occur depending on the cumulative stress factor characterizing a specific site. This is confirmed by a study [25] in which the degradation rates were modeled in two benchmark climates (humid and tropical and hot and dry). Again the computed rates are very similar.

V. Conclusion

The PLR for different technologies was calculated in different climates. The outliers were discussed and where possible an explanation for their behavior was given. After removing the outliers, for technologies which are not affected by metastability, no difference was observed that could be directly linked to the climate when comparing the PLRs values and accounting for the related uncertainties. Nevertheless more comparative studies in different climate zones are needed. Furthermore, the average PLR for each technology was computed. These rates can be seen as representative for the module type in question.

As a conclusion from these findings, it can be assumed that results from a single plant, e.g., [9] or [11], can be generalized due to so far minimal differences because of the climate. It is possible that in a later date, the difference will grow as the activation energy for different degradation modes will be reached at a different point in time because of the different stress factors. In this study, technologies were selected that were present at different sites. At all sites, the data and monitoring systems were managed carefully and thus a high quality of these results is expected. In this paper, the data were selected by detailed knowledge of the plant and monitoring system maintenance. Additional work on data of lower quality based on statistics will be performed. Then, failures are intrinsically included in PLR giving rise to the need for statistical filtering methods. These filtering methods need to distinguish between monitoring problems and actual PLR rate values.

In future work, the authors are planning to analyze some of the stress factors, which have an impact on the creation of defects. These include total amount of irradiance, average temperature, and UV exposure.

Acknowledgments

The authors would like to thank the Department of Innovation, Research and University of the Autonomous Province of Bozen/Bolzano for covering the Open Access publication costs.

References

[1] D. C. Jordan, S. R. Kurtz, K. VanSant, and J. Newmiller, "Compendium of photovoltaic degradation rates," *Prog. Photovolt.: Res. Appl.*, vol. 24, no. 7, pp. 978–989, Jul. 2016, doi: 10.1002/pip.2744.

[2] D. Jordan, J. Wohlgemuth, and S. Kurtz, "Technology and climate trends in PV module degradation," in *Proc. 27th Eur. Photovolt. Solar Energy Conf. Exhib.*, Frankfurt, Germany, 2012, pp. 3118–3124.

[3] G. Belluardo, M. Pichler, D. Moser, and M. Nikolaeva-Dimitrova, "One-year comparison of different thin film technologies at Bolzano airport test installation," in *Fuelling the Future: Advances in Science and Technologies for Energy Generation, Transmission and Storage*, A. Mendez-Vilas, Irvine, CA, USA: Universal-Publishers, 2012.

[4] L. Fanni, M. Giussani, M. Marzoli, and M. Nikolaeva-Dimitrova, "How accurate is a commercial monitoring system for photovoltaic plant?" *Progr. Photovolt.: Res. Appl.*, vol. 22, no. 8, pp. 910–922, 2014.

[5] D. Bertani, S. Guastella, G. Belluardo, and D. Moser, "Long term measurement accuracy analysis of a commercial monitoring system for photovoltaic plants," in *Proc. IEEE Workshop Environmental, Energy, Structural Monitoring Syst.*, 2015, pp. 84–89.

[6] IEC61724-1:2017(E), "Photovoltaic system performance—Part 1: Monitoring," 2017.

[7] G. Makrides, B. Zinsser, M. Schubert, and G. E. Georghiou, "Energy yield prediction errors and uncertainties of different photovoltaic models," *Prog. Photovolt.: Res. Appl.*, vol. 21, no. 4, pp. 500–516, Nov. 2011.

[8] M. C. Peel, B. L. Finlayson, and T. A. McMahon, "Updated world map of the Koppen-Geiger climate classification," *Hydrol. Earth Syst. Sci.*, vol. 11, no. 5, pp. 1633–1644, 2007. [Online]. Available: https://hal.archives-ouvertes.fr/hal-00298818

[9] P. Ingenhoven, G. Belluardo, and D. Moser, "Comparison of statistical and deterministic smoothing methods to reduce the uncertainty of performance loss rate estimates," *IEEE J. Photovolt.*, vol. 8, no. 1, pp. 224–232, Jan. 2018.

[10] R. J. Hyndman and G. Athanasopoulos, *Forecasting: Principles and Practice*. Melbourne, Australia: OTexts, Oct. 2013.

[11] A. Phinikarides, G. Makrides, B. Zinsser, M. Schubert, and G. E. Georghiou, "Analysis of photovoltaic system performance time series: Seasonality and performance loss," *Renew. Energy*, vol. 77, pp. 51–63, 2015.

[12] R. B. Cleveland, W. S. Cleveland, J. E. McRae, and I. Terpenning, "STL: A seasonal-trend decomposition procedure based on loess," *J. Official Statist.*, vol. 5, no. 1, pp. 3–33, Jan. 1990. [Online]. Available: https://www.scienceopen.com/document?vid=be074647-46c0-4ba9-991e-3124fbf63ed1

[13] *Curve Fitting Toolbox User's Guide*. The MathWorks, Inc, 2015. [Online]. Available: https://www.mathworks.com/help/pdf_doc/curvefit/curvefit.pdf

[14] A. Trapletti and K. Hornik, *Tseries: Time Series Analysis and Computational Finance*, 2017, r package version 0.10-38. [Online]. Available: https://CRAN.R-project.org/package=tseries

[15] R Core Team, *R: A Language and Environment for Statistical Computing*, R Foundation for Statistical Computing, Vienna, Austria, 2013. [Online]. Available: http://www.R-project.org/

[16] A. Kyprianou, A. Phinikarides, G. Makrides, and G. E. Georghiou, "Definition and computation of the degradation rates of photovoltaic systems of different technologies with robust principal component analysis," *IEEE J. Photovolt.*, vol. 5, no. 6, pp. 1698–1705, Nov. 2015.

[17] G. Belluardo *et al.*, "Novel method for the improvement in the evaluation of outdoor performance loss rate in different PV technologies and comparison with two other methods," *Solar Energy*, vol. 117, pp. 139–152, Jul. 2015, doi: 10.1016/j.solener.2015.04.030

[18] C. R. Osterwald *et al.*, "Comparison of degradation rates of individual modules held at maximum power," in *Proc. IEEE 4th World Conf. Photovolt. Energy Conf.*, May 2006, vol. 2, pp. 2085–2088.

[19] S. Boulhidja and A. Mellit, "Performance degradation of CIGS photovoltaic modules by light soaking and reverse bias," in *Proc. 4th Int. Conf. Electr. Eng.*, Dec. 2015, pp. 1–4.

[20] S. Dongaonkar, E. Sheets, R. Agrawal, and M. A. Alam, "Reverse stress metastability of shunt current in CIGS solar cells," in *Proc. 38th IEEE Photovolt. Spec. Conf.*, Jun. 2012, pp. 000868–000872.

[21] T. J. Silverman, L. Mansfield, I. Repins, and S. Kurtz, "Damage in monolithic thin-film photovoltaic modules due to partial shade," *IEEE J. Photovolt.*, vol. 6, no. 5, pp. 1333–1338, Sep. 2016.

[22] I. Repins and T. J. Silverman, "Shadows from people and tools can cause permanent damage in monolithic thin-film Photovoltaic modules," in *Proc. 33rd Eur. Photovolt. Solar Energy Conf. Exhib.*, Nov. 2017, pp. 1422–1426.

[23] R. Dubey *et al.*, "Comprehensive study of performance degradation of field-mounted photovoltaic modules in India," *Energy Sci. Eng.*, vol. 5, no. 1, pp. 51–64, Feb. 2017, doi: 10.1002/ese3.150.

[24] K. Radouane, M. Van Iseghem, C. Duchayne, and B. Braisaz, "PV aging model applied to several meteorological conditions," in *Proc. 29th Eur. Photovolt. Solar Energy Conf. Exhib.*, Nov. 2014, pp. 2303–2309.

[25] N. C. Park, W. W. Oh, and D. H. Kim, "Effect of temperature and humidity on the degradation rate of multicrystalline silicon photovoltaic module," *Int. J. Photoenergy*, vol. 2013, Art. no. 925280, doi: 10.1155/2013/925280.